Accepted Manuscript

Standardization proposal of soft tissue artefact description for data sharing in human motion measurements

Andrea Cereatti, Tecla Bonci, Massoud Akbarshahi, Kamiar Aminian, Arnaud Barré, Mickael Begon, Daniel L. Benoit, Caecilia Charbonnier, Fabien Dal Maso, Silvia Fantozzi, Cheng-Chung Lin, Tung-Wu Lu, Marcus G. Pandy, Rita Stagni, Antonie J. van den Bogert, Valentina Camomilla

PII: S0021-9290(17)30100-8
DOI: http://dx.doi.org/10.1016/j.jbiomech.2017.02.004
Reference: BM 8124

To appear in: *Journal of Biomechanics*

Accepted Date: 11 February 2017

Please cite this article as: A. Cereatti, T. Bonci, M. Akbarshahi, K. Aminian, A. Barré, M. Begon, D.L. Benoit, C. Charbonnier, F.D. Maso, S. Fantozzi, C-C. Lin, T-W. Lu, M.G. Pandy, R. Stagni, A.J. van den Bogert, V. Camomilla, Standardization proposal of soft tissue artefact description for data sharing in human motion measurements, *Journal of Biomechanics* (2017), doi: http://dx.doi.org/10.1016/j.jbiomech.2017.02.004

Standardization proposal of soft tissue artefact description for data sharing in human motion measurements

Andrea Cereatti[1,2,3]*, Tecla Bonci[3,4], Massoud Akbarshahi[5], Kamiar Aminian[6], Arnaud Barré[6], Mickael Begon[7], Daniel L. Benoit[8], Caecilia Charbonnier[9], Fabien Dal Maso[7], Silvia Fantozzi[10], Cheng-Chung Lin[11,12], Tung-Wu Lu[11,13], Marcus G. Pandy[5], Rita Stagni[10], Antonie J. van den Bogert[14], Valentina Camomilla[3,15]

[1] POLCOMING Department, Information Engineering Unit, University of Sassari, Sassari, Italy
[2] Dept. of Electronics and Telecommunications, Politecnico di Torino, Torino, Italy
[3] Interuniversity Centre of Bioengineering of the Human Neuromusculoskeletal system, University of Rome "Foro Italico", Rome, Italy
[4] Life and Health Sciences, Aston University, Birmingham, United Kingdom
[5] Department of Mechanical Engineering, University of Melbourne, Victoria, Australia
[6] Laboratory of Movement Analysis and Measurement, Ecole Polytechnique Fédérale de Lausanne, Lausanne, Switzerland
[7] Laboratory of Simulation and Movement Modeling, Department of Kinesiology, University of Montreal, Montreal, Canada
[8] Faculty of Health Sciences, University of Ottawa, Ottawa, Canada
[9] Artanim Foundation, Medical Research Department, Geneva, Switzerland
[10] Department of Electric, Electronic and Information Engineering "Guglielmo Marconi" – DEI, University of Bologna, Italy
[11] Institute of Biomedical Engineering, National Taiwan University, Taiwan, ROC
[12] Department of Electronic Engineering, Fu-Jen Catholic University, Taiwan, ROC
[13] Department of Orthopaedic Surgery, School of Medicine, National Taiwan University, Taiwan, ROC
[14] Department of Mechanical Engineering, Cleveland State University, Cleveland, Ohio, USA
[15] Department of Movement, Human and Health Sciences, University of Rome "Foro Italico", Rome, Italy

* Tel: +39-3387854455, *E-mail:* acereatti@uniss.it

Word Count: 3944

Keywords: Human Movement Analysis, Kinematics, Soft Tissue Artefact, Stereophotogrammetry, Open Data

Abstract

Soft tissue artefact (STA) represents one of the main obstacles for obtaining accurate and reliable skeletal kinematics from motion capture. Many studies have addressed this issue, yet there is no consensus on the best available bone pose estimator and the expected errors associated with relevant results. Furthermore, results obtained by different authors are difficult to compare due to the high variability and specificity of the phenomenon and the different metrics used to represent these data. Therefore, the aim of this study was twofold: firstly, to propose standards for description of STA; and secondly, to provide illustrative STA data samples for body segments in the upper and lower extremities and for a range of motor tasks specifically, level walking, stair ascent, sit-to-stand, hip- and knee-joint functional movements, cutting motion, running, hopping, arm elevation and functional upper-limb movements. The STA dataset includes motion of the skin markers measured *in vivo* and *ex vivo* using stereophotogrammetry as well as motion of the underlying bones measured using invasive or bio-imaging techniques (i.e., X-ray fluoroscopy or MRI). The data are accompanied by a detailed description of the methods used for their acquisition, with information given about their quality as well as characterization of the STA using the proposed standards. The availability of open-access and standard-format STA data will be useful for the evaluation and development of bone pose estimators thus contributing to the advancement of three-dimensional human movement analysis and its translation into the clinical practice and other applications.

1. Introduction

The analysis of joint mechanics requires the estimation of both position and orientation (pose) of the bones which meet at a joint. However, due to muscle contraction, wobbling of soft tissues and skin stretching/sliding, the relative positions between the skin and the underlying bones changes over time during the execution of a given motor task. The relative movement between the skin and underlying bone is commonly referred to as soft tissue artefact (STA) and represents one of the main obstacles for obtaining accurate and reliable measurements of skeletal kinematics using skin-mounted markers and stereophotogrammetry or wearable sensors (Leardini et al., 2005; Peters et al., 2010). Various bone pose estimators have been proposed to reduce the impact of STA on estimates of joint kinematics, including least square methods (Camarn and Milburn, 2005), inertia methods (Andriacchi et al., 1998; Alexander and Andriacchi, 2001), optimal cluster model procedures (Chèze et al., 1995; Taylor et al., 2005), methods incorporating STA calibration procedures (Lucchetti et al., 1998; Cappello et al., 2005) and global optimization approaches (Andersen et al., 2009; Lu and O'Connor, 1999; Reinbolt et al., 2005). However, no consensus has been reached either on the best available estimator or on the maximum errors associated with these different methods (Barré et al., 2015; Benoit et al., 2007; Cereatti et al., 2006; Stagni et al., 2009).

There are several reasons for the lack of a consensus. First, STA quantification is a cumbersome, expensive, and time-consuming process which requires the determination of a virtually error-free bone pose using either invasive techniques such as pins inserted into the bones (Benoit et al., 2006; Cereatti et al., 2009; Dal Maso et al., 2015; Lafortune et al., 1992; Reinschmidt et al., 1997) or bio-imaging techniques such as fluoroscopy and magnetic resonance (MR) imaging (Bey et al., 2008; Garling et al., 2008; Guan et al., 2016; Stagni et al., 2005). The need for complex experimental set-ups and procedures (*e.g.* simultaneous recordings using different instrumentation and surgical intervention for insertion of bone

pins), expensive measurement systems (*e.g.* single/dual-plane fluoroscopy, MR imaging, and high resolution multi-camera systems) and highly-specific, multidisciplinary expertise (bioengineers, orthopaedics, and physiotherapists) may explain the relatively small sample sizes and diverse experimental datasets available in the literature. Second, differences observed in the STA characteristics may be due to experimental inaccuracies resulting from intrinsic measurement limitations that have affected both the spatial and temporal resolution of the measured error-free bone pose (Peters et al., 2010; Ramsey et al., 2003; Tersi et al., 2013). Third, there is ample evidence in the literature to suggest that STA depends on several factors such as subject anthropometry, the body segment on which a particular marker is located, the location of that marker, and the type of activity performed (Barré et al., 2013; Cappello et al., 2005; Cappozzo et al., 1996; Peters et al., 2010). These factors result in the high variability and specificity observed in the STA patterns and amplitudes. Therefore, when STA data are used, for example, to assess the performance of a specific bone pose estimator or to perform comparative evaluations, it is crucial to provide a thorough description of the experimental data used as input for the analysis (*e.g.* number of markers forming the cluster, marker location, description of the motor task analysed and of the subject characteristics). It should be noted that the aforementioned STA variability and specificity have impeded the development of subject-specific models for STA compensation, applicable and effective under different experimental conditions. Lastly, different metrics have been used in the literature to describe the STA amplitude making it difficult to direct compare the results (Dumas et al., 2014; Peters et al., 2010).

The present study addresses the aforementioned limitations by proposing a standardization of the metrics for STA description at the marker level and providing an exemplar STA dataset organized in a standardized format for STA data exchange. This dataset is comprised of STA data relative to different body segments in the upper and lower extremities, different subjects,

and motor tasks (walking, step ascent, sit-to-stand, hip and knee joint functional movements, cutting motion, running, hopping, arm elevation and functional upper limb movements). The dataset was created by compiling the STA data published by various investigators from different laboratories using different techniques. It includes the motion of the skin marker measured using stereophotogrammetry *in vivo* and *ex vivo* as well as that of the underlying bones using invasive or bio-imaging techniques (i.e., X-ray fluoroscopy or MRI) for various motor tasks in single trials of single selected subjects or specimens (data sample) for various motor tasks. Each data sample is accompanied with a thorough description of the material and methods used, information about the data quality when available in the original studies, and a characterization of the STA characteristics using the proposed standards.

2. Material and Methods

2.1 Metrics for STA description

Consider a skin marker attached to a generic body segment, and let $\mathbf{p}_i$ be its position vector in the relevant bone-embedded anatomical coordinate system (ACS) at a given sampled instant of time *i*. During the motion of the body segment, $\mathbf{p}_i$ will change due to the deformation of the soft tissues. The variation of $\mathbf{p}_i$ over time represents the STA affecting the skin marker. In other words, the problem of the STA characterization is equivalent to the description of the change over time of a vector in a 3D Euclidean space.

An effective statistical description of the STA should include information on both amplitude and direction. For each given skin marker during a given motor task, the following quantities are defined over the *N* available observations over time:

Mean position vector: $\bar{\mathbf{p}} = \frac{1}{N}\sum_{i=1}^{N}\mathbf{p}_i \qquad i = 1,..,N$ (1)

Instantaneous displacement vector: $\mathbf{d}_i = \begin{pmatrix} d_{x,i} & d_{y,i} & d_{z,i} \end{pmatrix} = \mathbf{p}_i - \bar{\mathbf{p}}$ (2)

Root mean square amplitude: $\mathrm{rms}(d) = \sqrt{\frac{\sum_{i=1}^{N} \|\mathbf{d}\|_i^2}{N}}$ (3)

Root mean square amplitude components: $rmsd_c = \sqrt{\frac{\sum_{i=1}^{N} \mathrm{d}_{c,i}^2}{N}} \qquad c = x, y, z;$ (4)

Peak-to-peak amplitude: $\Delta p_{\max} = \max\left(\left\|\mathbf{p}_i - \mathbf{p}_j\right\|\right)$ (5)

Peak-to peak components:

$\Delta p_c = \max(p_{c,i}) - \min(p_{c,j}) \qquad i = 1,..,N;\ j = 1,..,N;\ c = x, y, z$ (6)

The parameter *rmsd* provides a mean description of the STA amplitude in 3D space whereas the parameters $rmsd_c$ (with c=x,y,z) describe the mean STA amplitude along each axis of the ACS. In addition, $\Delta p_{\max}$ and Δp_c (with c=x,y,z) represent the maximum variation of $\mathbf{p}_i$ in 3D space and along each axis of the ACS, respectively. Both the root mean square (RMS) amplitude *rmsd* and the peak-to-peak amplitude $\Delta p_{\max}$ do not depend on the definition of the ACS (Grimpampi et al., 2014) whereas $rmsd_c$ and Δp_c do.

In summary, the STA affecting a selected skin marker during a given motor task can be described by the following eight parameters:

- *rmsd* and $\Delta p_{\max}$ which describe the "mean" and "maximum" STA amplitude.

- $rmsd_c$ and Δp_c (with c=x,y,z) which provide information about the STA direction (6 parameters).

2.2 Description of the experimental data samples

The present study incorporates the largest number of STA data available in the literature; whenever possible, we have included data collected by different authors for the same motor task to increase the heterogeneity and completeness of the database. The inclusion criteria were as follows: a) sufficiently detailed description of the experimental methodology

employed for data collection; b) use of technically sound and validated techniques to obtain the ground truth bone pose; c) dynamic trials; d) availability of the time-variant anatomical coordinate system (ACS) pose and of the skin marker trajectories with respect to the ACS during the analysed motor task; e) willingness to share data.

For the sake of completeness, the data sample provided by Akbarshahi et al. (2010) was included, even though it does not fully satisfy the aforementioned criteria (only the relevant joint angle histories are reported but not the ACS poses during time).

For the convenience of data users, the following information is summarized and provided for each STA data samples as Supplementary Material A (section 2).

a) *Data sample name and scientific article(s) of reference*;

b) *Subject or specimen characteristics*: information about sex, age, mass, height, body mass index;

c) *Motor task description*: information aimed at describing the motor task analyzed (e.g. type of motion, gait speed, range of joint motion, tread and rise when step or seat are used, type of footwear.);

d) *Experimental data description*: list of the body segments analysed, skin marker locations, and anatomical landmarks used;

e) *Anatomical coordinate systems definitions (ACS);*

f) *Measurement specifications*: description of the measurement systems and techniques used to process the position data (e.g. number of cameras, capture volume, sample frequency, measurement accuracy);

g) *Ground truth*: description of the technique used to determine the ground truth bone pose (e.g. measurement accuracy, procedures for calibration, registration, and synchronization between instruments);

h) *STA characterization*: for each marker, a description of the relevant STA is provided according to the proposed metrics. The dispersion of each STA parameter over all available markers is described using a five-number summary technique (minimum, lower quartile, median, upper quartile, and maximum).

Data are presented according to a lexicon described in Supplementary Material A (section 3). The lexicon was devised to store the data in a common data format, relative to position and orientation of upper or lower limb body segments while aiming at a complete description of the kinematics of a motor task. This choice allows a user to obtain a final data representation according to his/her interests, without knowing the experimental set-up of the laboratory where data were acquired. The lexicon is detailed in terms of:

- Data set storing description (Dataset name; Data information; Measurement Units).
- Subject description (Subject name; Subject information; Warning; Subject data).
- Legend tables (owner, motor task, footwear, pathology, side, segment, anatomical landmarks)

For some variables and parameters, to be included in the file, standard names were used (listed in *ad hoc* tables). The data structure is depicted in Figure 1. For the sake of usability, each data sample is organized using both a MATLAB structure (MathWorks) and an open textual data format (XML) and made available as Supplementary Material “dataSample”. Further details on the structure of the data can be found in Supplementary Material A (section 3).

FIGURE 1 ABOUT HERE

An overview of the 31 data samples available, grouped in terms of body segment and motor task, is given in Table 1. A detailed description of each data sample is provided in Supplementary Material A (section 2).

TABLE 1 ABOUT HERE

2.3 Data processing

Skin marker trajectories of each data sample were represented in the relevant ACS. The coordinates of the anatomical landmarks in the ACS were also provided when these data were available. A minimal amount of adjustments were made to the original raw data as described below:

- *Gap filling*: marker trajectories with gaps smaller than 0.35 s were filled using a partial Procrustes superimposition approach (Grimpampi et al., 2014), while trajectories showing gaps larger than 0.35 s were removed (gap filling not reliable). For these data samples, both original data and data after gap filling were provided.

For the data sample *Overground walking* no gap filling was implemented since all the skin markers showed a gap of 0.43 s due to overlapping of the knee joints on the fluoroscopic image during the gait cycle.

- *Data Filtering*: no further data processing was performed in addition to the original filtering specified, if performed, in the Supplementary material;

- *Coordinate system transformations*: the original ACSs were rotated whenever necessary to consistently express the skin marker trajectories with respect to the anatomical directions in accordance to the proposed Lexicon (x: anterior (+)-posterior, y: superior (+)-inferior, z: right (+)-left anatomical directions; supplementary material A, section 3).

After these preliminary data processing steps, the skin marker trajectories represented in the relevant ACSs were used to compute the eight parameters proposed as a metrics for STA description. Relevant descriptive statistics were summarized with the five–number summary technique (minimum, lower quartile, median, upper quartile, and maximum).

3. Results

An overall description of the STA mean and maximum amplitude computed over the available skin markers, as obtained from the different data samples according to the proposed metrics, is given in Table 2. The total number of skin markers varied greatly over the different data samples, between 4 and 35 for the thigh, between 3 and 26 for the shank, between 4 and 7 for the arm and between 8 and 57 for the scapula. A detailed description of the STA affecting each skin markers can be found in the Supplementary Material A (section 2).

All data samples described in Table 2 are made available for download and include information about the positions of the skin markers in the relevant ACS and the position and orientation of the ACS during the dynamic trials. Each data sample is thoroughly described and organized according to a well-documented structure to facilitate data sharing (Figure 1).

TABLE 2 ABOUT HERE

4. Discussion

The aim of this work was to propose standards for the description of STA and for data exchange and to provide an exemplar dataset that can support the development and evaluation of methods used to accurately estimate bone pose.

According to the proposed metrics, STA affecting each single marker is described through eight parameters, specifically, the mean and maximum amplitudes (*rmsd* and $\Delta p_{\max}$) and their

relevant variations along ACS directions ($rmsd_c$ and Δp_c, with $c=x,y,z$). It is important to note that the parameter *rmsd* does not depend on the definition of the ACS because it represents the RMS of the marker instantaneous displacement with respect to its mean position in the ACS for the specific motor task analyzed. In contrast, in previous studies the STA affecting the skin marker trajectory has often been defined as its local displacement from a reference position fixed in the ACS. This reference position was possibly chosen as the position of the marker at a given time, for example, at the beginning of an experiment or while the subject assumes a standard static posture (Grimpampi et al., 2014). The latter description can be useful and practical when applying methods for STA compensation based on the identification of the anatomical landmarks in given configurations (*e.g.* double anatomical calibration technique) (Cappello et al., 1996). However, when the primary aim is to characterize STA amplitude, the mean position is preferred since it is independent of the choice of initial reference position, thus facilitating a comparison of the STA amplitude among different experiments (Fig. 2).

FIGURE 2 ABOUT HERE

The STA dataset made available for download was created from selected data samples obtained from previously published studies (Supplementary Material "dataSample"). STA measurements obtained in different studies on various body segments and motor tasks using different techniques are presented here for the first time using standardized metrics, thus eliminating inconsistencies arising from the selection of different descriptions or reference positions for the STA definition.

It is important to note that each data sample made available for download refers to single subject/specimen performing a single trial. Due to the arbitrary selection of the experimental

data sample, the limited number of subjects/specimens for each motor task and the variability in the marker locations, the present dataset is not intended to provide a statistical description of the STA characteristics. Consequently, a comparison of the STA characteristics among the different data samples (Table 2) is only adequate for preliminary analysis, and for verifying the internal consistency of STA observation in human subjects.

In accordance with previous investigations (Cappozzo et al., 1996; Peters et al., 2010), STAs affecting the thigh markers were highly variable for the different motor tasks analysed, but in general were larger than those affecting the shank. The only exceptions related to the task of *knee extension against gravity*, performed in an up-right posture with the hip flexed at approximately 45 deg (Stagni et al., 2005), and the task of *knee flexion* (Akbarshahi et al., 2010). In these studies, both STA *rmsd* and $\Delta p_{\max}$ values were slightly, but consistently, larger for the shank compared to the thigh (*knee extension against gravity:* median *rmsd* values = 11.5 mm and 9.2 mm for shank and thigh, respectively; *knee-flexion*: median *rmsd* values = 8.6 mm and 7.4 mm for shank and thigh, respectively). These results suggest that differences in experimental settings and in the motor task analyzed may have a strong influence in determining STA magnitude. In fact, the aforementioned tasks involved large rotations at the knee joint with the hip joint locked. This circumstance could cause substantial sliding of the skin markers in proximity of the knee joint, regardless of whether they belong to the thigh or the shank.

Thigh STA amplitudes observed during walking (*over-ground* and *treadmill walking*) in three out of four different data samples (Barré et al., 2013; Benoit et al., 2006; Tsai et al., 2009) were consistent, exhibiting median *rmsd* values in the range of 7.6-8.4 mm and median $\Delta p_{\max}$ values in the range of 23.4-28.4 mm. Larger STA amplitudes were observed for the *treadmill walking* data collected by Akbarshahi et al., 2010 (median *rmsd* = 13.7 mm and median $\Delta p_{\max}$ equal to 41.2 mm). A larger variability was observed for the STA affecting the

shank markers during walking (median *rmsd* in the range of 2.4-7.5 mm and median Δp_{max} values in the range of 8.4-26.3 mm).

With respect to the lower limb, the largest STAs were observed for the thigh markers during the *Sit-to-stand* and *Step-up* exercises investigated by Stagni et al., (2005) and Tsai et al., (2009) (median Δp_{max} values up to 72.3 mm and 46.5 mm for *Sit-to-stand* and *Step-up*, respectively). These results may be explained by the effects of the skin sliding and muscle contraction components, which are expected to be considerable during tasks involving large and simultaneous joint excursion at the hip and knee joints. Furthermore, during *Sit-to-stand*, soft tissue deformation due to the compression of the seat during the sitting phase may cause an increase of the STA amplitude affecting the markers proximally and posteriorly located on the thigh segment.

The differences observed in STA amplitudes for the data samples may also be explained by the different numbers of markers and their disparate locations on the body segment, together with differences in age and body mass index of the subjects.

STAs affecting the upper limb during basic arm movements (flexion-extension and ab-adduction) highly varied between the two studies analysed (median *rmsd* in the range of 4.1-15.3 mm and median Δp_{max} in the range of 11.8-41.2 mm for the arm) (Charbonnier et al., 2014; Dal Maso et al., 2015, 2014). Substantially larger STA amplitudes were observed for the scapula, which exhibited median *rmsd* values in the range 8.5-21.0 mm and median Δp_{max} values in the range 27.8-56.8 mm (Charbonnier et al., 2014; Dal Maso et al., 2015, 2014). The discrepancies observed between the STA amplitudes reported here may be due to the anthropometric differences in height, mass, and muscle volume between the two subjects analyzed (Cereatti et al., 2015; Charbonnier et al., 2014; Dal Maso et al., 2015, 2014). The largest STAs were observed for the markers attached to the scapula during the execution of

sport activities such as *Ball throwing* (median *rmsd* = 34.8 mm; median Δp_{max} = 111.3 mm) and *Punching* (median *rmsd* = 19.8 mm; median Δp_{max} = 63.4 mm) (Dal Maso et al., 2015). These results confirmed the well-known difficulties related to the measurement of scapular motion (Anglin and Wyss, 2000), especially in sporting related activities such as throwing (Myers et al., 2015).

The present database includes STA measurements for the thigh, shank, arm and scapula. We acknowledge that markers positioned on the ASISs are susceptible to large STA (Hara et al., 2014), however it was not possible to include data on the pelvic STA because of the absence of data recorded under dynamic conditions.

The STA data included in the open dataset were obtained using a variety of gold standard methods. Each technique has its own limitations (*e.g.*, pins may constrain skin movement; scapula is difficult to track using fluoroscopy) which involve measurement errors, the magnitudes of which are difficult to predict and quantify (Peters et al., 2010). For this reason, we have included in the final dataset the largest number of STA data samples from different sources, even if these data were collected during similar or identical motor tasks.

The data presented in the Supplementary Material includes, for each sampled time instant, both the positions of the skin markers in the relevant ACS and the position and orientation of the ACS with respect to a global coordinate system during related dynamic trials. Through simple rigid body transformations, it is possible to express the marker data in any arbitrary selected coordinate system and to compute joint angular kinematics according to any preferred rotation sequence (Senk et al., 2006; Wu et al., 2002; Wu et al:, 2005). Whilst representing the data in this way makes it applicable to a wide range of applications, the one exception to the aforementioned data format is the study by Akbarshahi et al. (2010) which contains the marker trajectories in the ACS and the relevant joint angle histories, not the ACS poses over time. The latter description, although partial, could be useful for instance to

investigate possible correlation between STA and joint angular kinematics (Camomilla et al., 2013; Cappozzo et al., 1996).

There are limitations of this study that must be acknowledged. First, the present work is concerned only with STA affecting individual markers, but not at marker cluster level. However, a similar analysis could be performed, using the provided skin marker data, to describe the effect of the STA on cluster position and orientation (rigid motion), and size and shape (non-rigid motion) (Andersen et al., 2012; Benoit et al., 2015; De Rosario et al., 2012; Dumas et al., 2014; Dumas and Chèze, 2009; Grimpampi et al., 2014). Second, we did not include data on STA effect on measures performed with wearable measurement units markers attached to a rigid shell (Manal et al., 2000). To authors' knowledge no information is available in the literature about STA affecting wearable measurement units. Nevertheless, the STA data provided in this study could be used to preliminary devise simulations of the rigid motion component due to STA affecting the segment location where the wearable measurement units or rigid shells would be attached. However, these data do not allow to describe the inertial effects of the mass of the wearable measurement units or rigid shells and the effects of the different fixing techniques. These factors would surely affect the magnitude and frequency content of the STA. Future work in this direction is recommended since wearable measurement units are becoming increasingly popular for kinematic measurements.

We expect that the verification of STA data performed in the present study together with the proposed standardization and sharing of the data will promote the following outcomes: first, it will enable a more effective and reliable comparison of existing methods for STA compensation (Alexander and Andriacchi, 2001; Cappello et al., 1996; Chéze et al., 1995; Peters et al., 2010; Solav et al., 2015; Stagni et al., 2009); second, it will facilitate the creation and validation of novel bone pose estimators eventually embedding models of the STA that can capture its specificity (Richard et al., 2012); and third, it will lead to an evidence-based

consensus on the level of accuracy of the marker-based stereophotogrammetry methods for estimating the pose of different bony segments.

Furthermore, when more sample trials and subjects will be collected and made available, it could be possible to develop statistical parametric model of the STA in humans and to validate these for different motor tasks and anthropometric differences to partially remove STA from skin markers or sensors (Andersen et al., 2012; Bonci et al., 2014; Camomilla et al., 2015; van Weeren et al., 1992).

Finally, we hope that by providing easy access to data describing the deformation of body segments during movement, researchers from different backgrounds and disciplines will be better motivated to challenge the STA issue with new ideas and methods for the advancement of three-dimensional human movement analysis and its translation into the clinical practice and other applications (Hicks et al., 2015).

Conflicts of interest

There are no conflicts of interest.

Data use policy

We request that the present study be specifically and clearly acknowledged when data sets or data samples are used for data analyses and visualizations in publications, posters, oral presentations, reports, Web pages, and any other types of scientific media. Please cite also the relevant original studies of each used specific data samples

Acknowledgements

This work was partly supported by a Grant from the Università di Roma "Foro Italico" (call PR_15) and the "Fondation de soutien à la recherche dans le domaine de l'othorpédie-traumatologie".

References

Akbarshahi, M., Schache, A.G., Fernandez, J.W., Baker, R., Banks, S., Pandy, M.G., 2010. Non-invasive assessment of soft-tissue artifact and its effect on knee joint kinematics during functional activity. J. Biomech. 43, 1292–1301.

Alexander, E.J., Andriacchi, T.P., 2001. Correcting for deformation in skin-based marker systems. J. Biomech. 34, 355–361.

Andersen, M.S., Benoit, D.L., Damsgaard, M., Ramsey, D.K., Rasmussen, J., 2010. Do kinematic models reduce the effects of soft tissue artefacts in skin marker-based motion analysis? An in vivo study of knee kinematics. J. Biomech. 43, 268-273.

Andersen M.S., Damsgaard, M., Rasmussen J., 2009. Kinematic analysis of over-determinate biomechanical systems. Comput Methods Biomech Biomed Engin. 12, 371-84.

Andersen, M.S., Damsgaard, M., Rasmussen, J., Ramsey, D.K., Benoit, D.L., 2012. A linear soft tissue artefact model for human movement analysis: Proof of concept using in vivo data. Gait Posture 35, 606–611.

Andriacchi, T.P., Alexander E.J., Toney M.K., Dyrby C., Sum, J., 1998. A point cluster method for in vivo motion analysis: applied to a study of knee kinematics. J. Biomech. Eng. 120, 743-9.

Anglin, C., Wyss, U.P., 2000. Review of arm motion analyses. Proc. Inst. Mech. Eng. H. 214, 541–555.

Barré, A., Jolles, B.M., Theumann, N., Aminian, K., 2015. Soft tissue artifact distribution on lower limbs during treadmill gait: Influence of skin markers' location on cluster design. J. Biomech. 1–7.

Barré, A., Thiran, J.P., Jolles, B.M., Theumann, N., Aminian, K., 2013. Soft tissue artifact assessment during treadmill walking in subjects with total knee arthroplasty. IEEE Trans. Biomed. Eng. 60, 3131–3140.

Benoit, D.L., Ramsey, D.K., Lamontagne, M., Xu, L., Wretenberg, P., Renström, P., 2006. Effect of skin movement artifact on knee kinematics during gait and cutting motions measured in vivo. Gait Posture 24, 152–164.

Benoit, D.L., Ramsey, D.K., Lamontagne, M., Xu, L., Wretenberg, P., Renström, P., 2007. In vivo knee kinematics during gait reveals new rotation profiles and smaller translations. Clin. Orthop. Relat. Res. 454, 81–88.

Benoit, D.L., Damsgaard, M., Andersen, M.S., 2015. Surface marker cluster translation, rotation, scaling and deformation: Their contribution to soft tissue artefact and impact on knee joint kinematics, J. Biomech. 48(10), 2124-2129.

Bey, M.J., Kline, S.K., Zauel, R., Lock, T.R., Kolowich, P.A., 2008. Measuring dynamic in-vivo glenohumeral joint kinematics: Technique and preliminary results. J. Biomech. 41, 711–714.

Bonci, T., Camomilla,V., Dumas, R., Chèze, L., Cappozzo, A., 2014. A soft tissue artefact model driven by proximal and distal joint kinematics. J.Biomech. 47(10), 2354–2361.

Carman, A., Milburn, P., 2006. Determining rigid body transformation parameters from ill conditioned spatial marker co-ordinates. J. Biomech. 39(10), 1778-86.

Camomilla, V., Cereatti, A., Chèze, L., Cappozzo, A., 2013. A hip joint kinematics driven model for the generation of realistic thigh soft tissue artefacts. J. Biomech. 46, 625–630.

Camomilla, V., Bonci, T., Dumas, R., Chèze, L., Cappozzo, A., 2015. A model of the soft

tissue artefact rigid component. J. Biomech. 48, 1752–1759.

Cappello, A., Cappozzo, A., Palombara, P.F. La, Leardini, A., Bertani, A., 1996. Skin artefact compensation by double calibration in bone motion reconstruction. Proc. 18th Annu. Int. Conf. IEEE Eng. Med. Biol. Soc.

Cappello, A., Stagni, R., Fantozzi, S., Leardini, A., 2005. Soft tissue artifact compensation in knee kinematics by double anatomical landmark calibration: Performance of a novel method during selected motor tasks. IEEE Trans. Biomed. Eng. 52, 992–998.

Cappozzo, A., Catani, F., Leardini, A., Benedetti, M.G., Della Croce, U., 1996. Position and orientation in space of bones during movement: Experimental artefacts. Clin. Biomech. 11, 90–100.

Cereatti, A., Della Croce, U., Cappozzo, A., 2006. Reconstruction of skeletal movement using skin markers: comparative assessment of bone pose estimators. J. Neuroeng. Rehabil. 3, 7.

Cereatti, A., Donati, M., Camomilla, V., Margheritini, F., Cappozzo, A., 2009. Hip joint centre location: An ex vivo study. J. Biomech. 42, 818–823.

Cereatti, A., Rosso, C., Nazarian, A., DeAngelis, J.P., Ramappa, A.J., Croce, U. Della, 2015. Scapular motion tracking using acromion skin marker cluster: In vitro accuracy assessment. J. Med. Biol. Eng. 35, 94–103.

Charbonnier, C., Chagué, S., Kolo, F.C., Chow, J.C.K., Ladermann, A., 2014. A patient-specific measurement technique to model shoulder joint kinematics. Orthop. Traumatol. Surg. Res. 100, 715–719.

Chéze, L., Fregly, B.J., Dimnet, J., 1995. A solidification procedure to facilitate kinematic

analyses based on video system data. J. Biomech. 28, 879–884.

Dal Maso, F., Blache, Y., Raison, M., Lundberg, A., Begon, M., 2015. Glenohumeral joint kinematics measured by intracortical pins, reflective markers, and computed tomography: A novel technique to assess acromiohumeral distance. J. Electromyogr. Kinesiol. 1–8.

Dal Maso, F., Raison, M., Lundberg, A., Arndt, A., Begon, M., 2014. Coupling between 3D displacements and rotations at the glenohumeral joint during dynamic tasks in healthy participants. Clin. Biomech. 29, 1048–1055.

De Rosario, H., Page, A., Besa, A., Mata, V., Conejero, E. 2012. Kinematic description of soft tissue artifacts: quantifying rigid versus deformation components and their relation with bone motion. Med. Biol. Eng. Comput., 50(11), 1173-1181.

Dumas, R., Camomilla, V., Bonci, T., Chéze, L., Cappozzo, A., 2014. Generalized mathematical representation of the soft tissue artefact. J. Biomech. 47, 476–481.

Dumas, R., Chéze, L., 2009. Soft tissue artifact compensation by linear 3D interpolation and approximation methods. J. Biomech. 42, 2214–2217.

Garling, E.H., Kaptein, B.L., Mertens, B., Barendregt, W., Veeger, H.E.J., Nelissen, R.G.H.H., Valstar, E.R., 2008. Soft-tissue artefact assessment during step-up using fluoroscopy and skin-mounted markers. J Biomech. 41, 2332-5.

Grimpampi, E., Camomilla, V., Cereatti, A., De Leva, P., Cappozzo, A., 2014. Metrics for describing soft-tissue artefact and its effect on pose, size, and shape of marker clusters. IEEE Trans. Biomed. Eng. 61, 362–367.

Grood, E.S., Suntay, W.J., 1983. A joint coordinate system for the clinical description of

three-dimensional motions: application to the knee. J. Biomech. Eng. 105, 136–44.

Guan, S., Gray, H., Keynejad, F., Pandy, M.G., 2016. Mobile biplane X-ray imaging system for measuring 3D dynamic joint motion during overground gait. IEEE Transactions on Medical Imaging 35: 326-336.

Hara, R., Sangeux, M., Baker, R., McGinley, J., 2014. Quantification of pelvic soft tissue artifact in multiple static positions. Gait Posture 39, 712–717.

Hicks, J.L., Uchida, T.K., Seth, A., Rajagopal, A., Delp, S., 2015. Is my model good enough? Best practices for verification and validation of musculoskeletal models and simulations of human movement. J. Biomech. Eng. 137, 20905.

Lafortune, M.A., Cavanagh, P.R., Sommer, H.J., Kalenak, A., 1992. Three-dimensional kinematics of the human knee during walking. J. Biomech. 25, 347–357.

Leardini, A., Chiari, L., Della Croce, U., Cappozzo, A., 2005. Human movement analysis using stereophotogrammetry - Part 3. Soft tissue artifact assessment and compensation. Gait Posture 21, 212–225.

Lucchetti, L., Cappozzo A., Cappello, A,. Della Croce U., 1998. Skin movement artefact assessment and compensation in the estimation of knee-joint kinematics. J Biomech. 31, 977-84.

Lu, T.W., O'Connor, J.J., 1999. Bone position estimation from skin marker co-ordinates using global optimisation with joint constraints. J. Biomech. 32, 129–134.

Manal, K., McClay, I., Stanhope, S., Richards, J., Galinat, B., 1997. Comparison of surface mounted markers and attachment methods in estimating tibial rotations during walking: an in vivo study. Gait Posture 11, 38-45.

Myers, C.A., Laz, P.J., Shelburne, K.B., Davidson, B.S., 2015. A Probabilistic Approach to Quantify the Impact of Uncertainty Propagation in Musculoskeletal Simulations. Ann. Biomed. Eng. 43, 1098–1111.

Peters, A., Galna, B., Sangeux, M., Morris, M., Baker, R., 2010. Quantification of soft tissue artifact in lower limb human motion analysis: A systematic review. Gait Posture 31, 1–8.

Ramsey, D.K., Wretenberg, P.F., Benoit, D.L., Lamontagne, M., Németh, G., 2003. Methodological concerns using intra-cortical pins to measure tibiofemoral kinematics. Knee Surg. Sports Traumatol. Arthrosc. 11, 344–349.

Reinbolt, J.A., Schutte, J.F., Fregly, B.J., Koh, B.I., Haftka, R.T., George, A.D., Mitchell, K.H.,. 2005. Determination of patient-specific multi-joint kinematic models though two-level optimization. J Biomech. 38:621–626.

Reinschmidt,C., VanDenBogert, A.J., Nigg, B.M., Lundberg, A., Murphy,N., 1997. Effect of skin movement on the analysis of skeletal knee joint motion during running. J.Biomech. 30(7),729–732.

Richard V., Camomilla V., Cheze L., Cappozzo A., Dumas, R, 2012. Feasibility of incorporating a soft tissue artefact model in multi-body optimisation. Computer methods in biomechanics and biomedical engineering 15 (sup1), 194-196.

Senk M, Chèze L., 2006. Rotation sequence as an important factor in shoulder kinematics. Clin Biomech. 21, 1:S3-8.

Solav, D., Rubin, M.B., Cereatti, A., Camomilla, V., Wolf, A., 2015. Bone Pose Estimation in the Presence of Soft Tissue Artifact Using Triangular Cosserat Point Elements. Ann. Biomed. Eng.

Stagni, R., Fantozzi, S., Cappello, A., 2009. Double calibration vs. global optimisation: Performance and effectiveness for clinical application. Gait Posture 29, 119–122.

Stagni, R., Fantozzi, S., Cappello, A., Leardini, A., 2005. Quantification of soft tissue artefact in motion analysis by combining 3D fluoroscopy and stereophotogrammetry: A study on two subjects. Clin. Biomech. 20, 320–329.

Taylor, W.R., Ehrig, R.M., Duda, G.N., Schell, H., Seebeck, P., Heller, M.O., 2005. On the influence of soft tissue coverage in the determination of bone kinematics using skin markers. J. Orthop. Res. 23, 726–734.

Tersi, L., Barré, A., Fantozzi, S., Stagni, R., 2013. In vitro quantification of the performance of model-based mono-planar and bi-planar fluoroscopy for 3D joint kinematics estimation. Med. Biol. Eng. Comput. 51, 257–265.

Tsai, T.-Y., Lu, T.-W., Kuo, M.-Y., Hsu, H.-C., 2009. Quantification of Three-Dimensional Movement of skin markers relative to the underlying bones during functional activities. Biomed. Eng. Appl. Basis Commun. 21, 223–232.

van Weeren, P.R., van den Bogert, A.J., Barneveld A., 1992. Correction models for skin displacement in equine kinematics gait analysis, J. Equine Vet. Sci., 12, 178-192.

Wu, G., Siegler S., Allard P., Kirtley C., Leardini A., Rosenbaum D., Whittle M., D'Lima D.D., Cristofolini L., Witte H., Schmid O., Stokes I. 2002. ISB recommendation on definitions of joint coordinate system of various joints for the reporting of human joint motion--part I: ankle, hip, and spine. J. Biomech 35, 543-8.

Wu, G., van der Helm, F.C.T., Veeger, H.E.J., Makhsous, M., Van Roy, P., Anglin, C., Nagels, J., Karduna, A.R., McQuade, K., Wang, X., Wernerl, F.W., Buchholz, B., 2005.

ISB recommendation on definitions of joint coordinate systems of various joints for the reporting of human joint motion−Part II: shoulder, elbow, wrist and hand. J. Biomech 38, 981–992.

Captions to figures

Figure 1:

Schematic description of a data sample based on the MatLab data format. Provider and motor task names are reported in the data sample name. For each *data sample*, general information on the experimental set-up is reported (*info field*). The *subj field* contains specific information of the subject (*subject.info field*), warnings on experimental problems (*subject.warning field*), and data acquired during the trial (*subject.trial field*) which, in turn, contains data for the body segments involved (*e.g. pelvis, R_thigh, R_shank fields*). For each body segment, the following information are available: warnings on experimental problems (*e.g. R_thigh.warning field*), time variant marker coordinates provided in the anatomical coordinate system (*mrk field*), rotation matrix (*gRa field*) and translation vector (*gta field*) of the anatomical coordinate system provided in the global frame. Time invariant data are also given for anatomical landmarks provided in the anatomical coordinate system (*ALs field*).

Figure 2:

STA displacements of a skin-marker glued on the thigh segment during the completion of hip joint centre functional movement. The time histories are represented choosing (a) the beginning of the relevant experiment and (b) the mean position as reference position. The anterior-posterior (AP), superior-inferior (SI), and medial-lateral (ML) displacements are shown (anterior, superior and right directions are positive). The relevant hip joint kinematics is also shown (c). The kinematics is calculated according to the convention proposed by Grood and Suntay (1983). Continuous black line: flexion/extension (FE); grey thin line: abduction/adduction (AA); grey dotted line internal/external rotation (IE); flexion, abduction and internal rotation are positive.

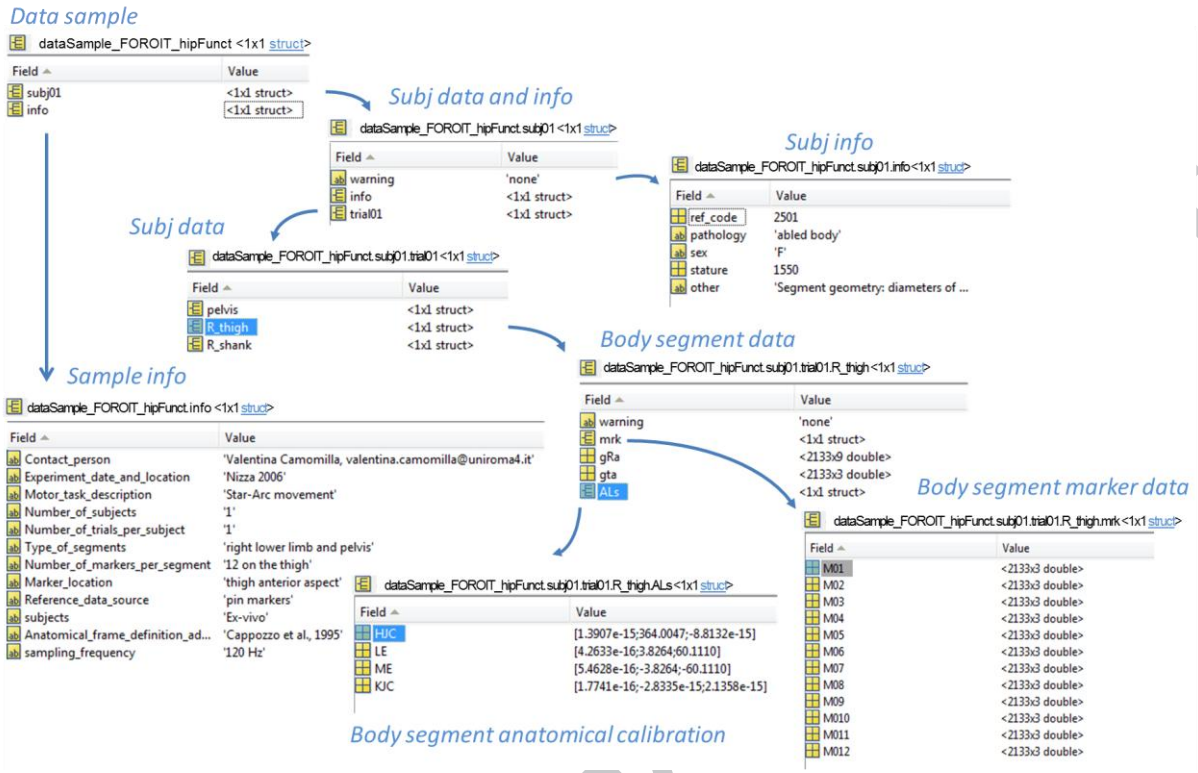

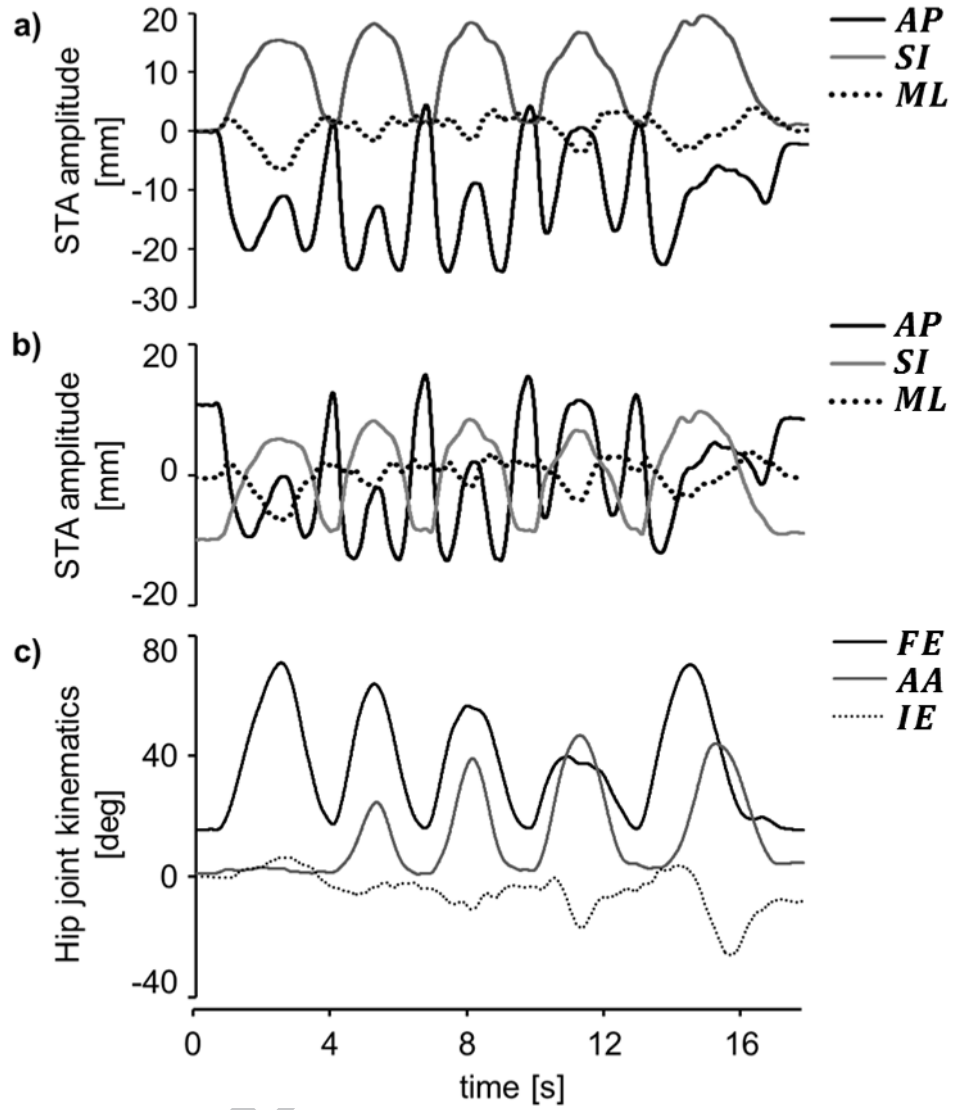

Tables

Table 1: STA dataset summary grouped by similar motor tasks. Reference papers, subject characteristics along with information on how the anatomical coordinate system (ACS) was defined and whether it is consistent with the ISB convention (Wu et al., 2002; Wu et al., 2005) or not, reference gold standard measure, marker number and body segment location are reported.

Motor Task	Reference papers	Data sample number	Subject Characteristics	Gender	BMI [kg/m^2]	Age [years]	Mass [kg]	Stature [m]	ACS definitions	Gold Standard	Skin-marker location
Hip joint centre functional movement (Star-Arc)	Camomilla et al., 2013 Cereatti et al., 2009	1	*ex vivo*	Female	NA	NA	NA	1.55	ISB convention ACSs obtained using technical skin markers and pointer on ALs	Pin data	12 on thigh
Hip axial rotation (knee extended)	Akbarshahi et al., 2010	2	adult able-bodied	Male	23.9	34	74	1.76	ACSs obtained using subject-specific MRI bone models	X-ray fluoroscopy unit	7 on thigh 3 on shank
Hip and knee flexion/extension	Bonci et al., 2014	3	*ex vivo*	Male	NA	NA	NA	1.62	ISB convention ACSs obtained using technical skin markers and pointer on ALs	Pin data	12 on thigh 4 on shank
Knee flexion	Akbarshahi et al., 2010	4	Adult able-bodied	Male	23.9	34	74	1.76	ACSs obtained using subject-specific MRI bone models	X-ray fluoroscopy unit	7 on thigh 3 on shank
Knee flexion/extension	Tsai et al., 2009	5	Adult able-bodied	Male	27.1	NA	84	1.76	ACSs obtained using subject-specific CT-scan bone models	Fluoroscopy system	6 on thigh 4 on shank
Knee extension against gravity	Stagni et al., 2005	6	Adult with total knee replacement	Female	24.1	67	58	1.55	ISB convention ACSs obtained using technical skin markers and pointer on ALs	Fluoroscopy system	19 on thigh 10 on shank
Treadmill walking	Akbarshahi et al., 2010	7	Adult able-bodied	Male	23.9	34	74	1.76	ACSs obtained using subject-specific MRI bone	X-ray fluoroscopy	7 on thigh 3 on shank

									models	unit	
Treadmill walking	Barré et al., 2014	8	Postero-stabilized total knee prosthesis patient	Female	23.3	75	65	1.67	ACSs defined on the knee prosthesis	Fluoroscopy system	80 over one lower limb
Overground walking	Tsai et al., 2009	9	Adult able-bodied	Male	27.4	NA	83	1.74	ACSs obtained using subject-specific CT-scan bone models	Fluoroscopy system	6 on thigh 4 on shank
Overground walking	Benoit et al., 2006	10	Adult able-bodied	Male	20.6	22	63	1.75	ACSs obtained using ALs identified on recorded RSA	Pin data	4 on thigh 4 on shank
Lateral cutting manoeuvres	Benoit et al., 2006	11	Adult able-bodied	Male	20.6	22	63	1.75	ACSs obtained using ALs identified on recorded RSA	Pin data	4 on thigh 4 on shank
Sit-to-stand	Tsai et al., 2009	12	Adult able-bodied	Male	27.4	NA	83	1.74	ACSs obtained using subject-specific CT-scan bone models	Fluoroscopy system	6 on thigh 4 on shank
Sit-to-stand	Kuo et al., 2011	13	Adult with posterior cruciate ligament retaining mobile bearing total knee replacement	Female	33.5	NA	87	1.61	ACSs obtained using subject-specific computer-aided design models of the knee prosthesis	Fluoroscopy system	6 on thigh 4 on shank
Sit-to-stand/stand-to-sit	Stagni et al., 2005	14	Adult with total knee replacement	Female	24.1	67	58	1.55	ISB convention ACSs obtained using technical skin markers and pointer on ALs	Fluoroscopy system	19 on thigh 10 on shank
Step-up	Akbarshahi et al., 2010	15	Adult able-bodied	Male	23.9	34	74	1.76	ACSs obtained using subject-specific MRI bone models	X-ray fluoroscopy unit	7 on thigh 3 on shank
Step-up	Tsai et al., 2011	16	Adult able-bodied	Male	27.4	NA	83	1.74	ACSs obtained using subject-specific CT-scan bone models .	Fluoroscopy system	6 on thigh 4 on shank
Step-up/down	Stagni et al., 2005	17	Adult with total knee replacement	Female	24.1	67	58	1.55	ISB convention ACSs obtained ACSs defined using technical skin markers and pointer on ALs	Fluoroscopy system	19 on thigh 10 on shank
Running	Reinschmidt et al.,1997	18	Adult able-bodied	Male					ACSs assumed to be parallel to the global frame during a standing trial	Pin data	5 on thigh 6 on shank
Hopping	Benoit et al., 2006 Andersen et al., 2012	19	Adult able-bodied	Male	20.6	22	63	1.75	ACSs obtained using ALs identified on recorded	Pin data	4 on thigh 4 on shank

									RSA		
Arm adduction	Dal Maso et al., 2015	20	Adult able-bodied	Male	20.9	27	57	1.65	ISB convention ACSs obtained using skin markers located on ALs.	Pin data	9 on scapula 7 on humerus 6 on thorax
Arm abduction	Dal Maso et al., 2015	21	Adult able-bodied	Male	20.9	27	57	1.65	ISB convention ACSs obtained using skin markers located on ALs.	Pin data	9 on scapula 7 on humerus, 6 on thorax
Arm abduction	Charbonnier et al., 2014	22	Adult able-bodied	Male	24.7	25	80	1.80	ISB convention ACSs obtained using ALs identified on the reconstructed bone models and MR images	Fluoroscopy at 30Hz	4 on upper arm 57 on the shoulder blade
Arm flexion	Dal Maso et al., 2015	23	Adult able-bodied	Male	20.9	27	57	1.65	ISB convention ACSs obtained using skin markers located on ALs.	Pin data	9 on scapula 7 on humerus, 6 on thorax
Arm flexion	Charbonnier et al., 2014	24	Adult able-bodied	Male	24.7	25	80	1.80	ISB convention ACSs obtained using ALs identified on the reconstructed bone models and MR images	Fluoroscopy at 30Hz	4 on upper arm 57 on the shoulder blade
Arm extension	Dal Maso et al., 2015	25	Adult able-bodied	Male	20.9	27	57	1.65	ISB convention ACSs obtained using skin markers located on ALs.	Pin data	9 on scapula 7 on humerus, 6 on thorax
Hair combing	Dal Maso et al., 2015	26	Adult able-bodied	Male	20.9	27	57	1.65	ISB convention ACSs obtained using skin markers located on ALs.	Pin data	9 on scapula 7 on humerus, 6 on thorax
Ball throwing	Dal Maso et al., 2015	27	Adult able-bodied	Male	20.9	27	57	1.65	ISB convention ACSs obtained using skin markers located on ALs.	Pin data	9 on scapula 7 on humerus, 6 on thorax
Eating	Dal Maso et al., 2015	28	Adult able-bodied	Male	20.9	27	57	1.65	ISB convention ACSs obtained using skin markers located on ALs.	Pin data	9 on scapula 7 on humerus, 6 on thorax
Gleno-humeral functional movement	Dal Maso et al., 2015	29	Adult able-bodied	Male	20.9	27	57	1.65	ISB convention ACSs obtained using skin markers located on ALs.	Pin data	9 on scapula 7 on humerus, 6 on thorax
Punching	Dal Maso et al., 2015	30	Adult able-bodied	Male	20.9	27	57	1.65	ISB convention ACSs obtained using skin markers located on ALs.	Pin data	9 on scapula 7 on humerus, 6 on thorax
Reaching the back	Dal Maso et al., 2015	31	Adult able-bodied	Male	20.9	27	57	1.65	ISB convention ACSs obtained using skin markers located on ALs.	Pin data	9 on scapula 7 on humerus, 6 on thorax

Table 2: First, second and third quartile of the standardized and common metrics used for STA characterization (i.e., "mean" and "maximum" STA amplitude, *rmsd* and Δp_{max}, respectively). Statistics performed over *n* skin-markers glued on the relevant segment. Values are calculated for the available data samples and grouped in terms of body segment and motor task.

			THIGH							SHANK						
			rmsd			Δp_{max}				*rmsd*			Δp_{max}			
			1st	2nd	3rd	1st	2nd	3rd	*n*	1st	2nd	3rd	1st	2nd	3rd	*n*
Lower Limb	*Hip joint centre functional movement (Star-Arc)*	Camomilla et al., 2013;Cereatti et al., 2009	4.4	(5.9)	7.1	17.6	(21.6)	25.9	12	–	–	–	–	–	–	–
		Akbarshahi et al., 2010	5.4	(6.7)	8.3	13.8	(17.7)	23.9	7	3.6	(3.7)	5.0	9.7	(10.1)	14.8	3
	Hip and knee flexion/extension	Bonci et al., 2014	5.7	(6.1)	6.4	15.1	(16.4)	17.7	12	1.2	(1.3)	1.4	4.1	(4.3)	4.4	4
	Knee flexion/extension	Akbarshahi et al., 2010	6.9	(7.4)	9.4	23.8	(25.5)	29.3	7	7.4	(8.6)	9.1	26.6	(31.7)	33.7	3
		Tsai et al., 2009	8.6	(9.2)	13.1	26.4	(27.6)	41.4	6	3.6	(5.0)	7.1	15.3	(18.7)	22.4	4
	Treadmill walking	Akbarshahi et al., 2010	10.1	(13.7)	14.9	30.0	(41.2)	44.7	7	7.1	(7.5)	8.2	18.0	(18.9)	20.1	3
		Barrè et al., 2014	6.8	(8.4)	9.7	23.4	(28.4)	32.7	35	2.5	(2.7)	2.9	10.0	(12.0)	14.1	26
	Overground walking	Tsai et al., 2009	7.3	(8.0)	9.3	21.3	(23.4)	27.3	6	2.4	(2.4)	2.4	7.9	(8.4)	8.7	4
		Benoit et al., 2006	6.3	(7.6)	8.6	22.0	(24.0)	24.3	4	3.9	(4.5)	5.0	22.2	(26.3)	28.7	4
	Lateral cutting manoeuvres	Benoit et al., 2006	6.5	(7.3)	8.1	19.5	(22.2)	26.5	4	2.1	(2.4)	2.6	6.2	(7.1)	7.9	4
	Sit-to-stand	Tsai et al., 2009	12.0	(12.9)	13.9	32.2	(35.3)	38.6	6	1.8	(2.2)	3.5	5.4	(7.2)	11.1	4
		Stagni et al., 2005	22.9	(25.3)	27.7	65.4	(72.3)	75.7	19	7.3	(7.6)	8.0	27.7	(29.1)	29.5	10
		Kuo et al., 2011	7.4	(8.0)	12.0	21.7	(22.2)	33.3	6	2.6	(3.0)	3.9	9.6	(11.4)	13.7	4
	Step-up	Akbarshahi et al., 2010	12.0	(12.4)	12.7	33.5	(34.8)	37.2	7	6.6	(7.6)	8.1	22.4	(26.4)	27.6	3
		Tsai et al., 2011	14.8	(15.1)	18.6	39.7	(46.5)	47.3	6	4.5	(5.0)	6.1	13.4	(15.6)	18.2	4
		Stagni et al., 2005	12.1	(14.9)	16.1	32.7	(41.8)	46.9	19	7.4	(7.5)	8.0	27.2	(28.5)	29.4	10
	Knee extension against gravity	Stagni et al., 2005	7.3	(9.2)	10.4	24.0	(26.7)	31.4	19	10.8	(11.5)	12.2	31.3	(32.5)	33.3	10
	Running	Reinschmidt et al.,1997	6.0	(6.9)	7.7	15.4	(21.1)	25.6	5	4.2	(4.7)	5.4	11.9	(12.8)	14.4	6
	Hopping	Andersen et al., 2012	3.5	(4.1)	4.7	16.1	(18.3)	19.7	4	1.4	(1.7)	1.8	11.9	(15.2)	17.9	4

			ARM							SCAPULA						
			rmsd			Δp_{max}				*rmsd*			Δp_{max}			
			1st	2nd	3rd	1st	2nd	3rd	*n*	1st	2nd	3rd	1st	2nd	3rd	*n*
Upper Limb	*Arm adduction*	Dal Maso et al., 2015	3.9	(4.1)	6.0	11.2	(11.8)	20.0	7	18.2	(19.9)	21.4	50.9	(54.0)	57.7	8
	Arm abduction	Dal Maso et al., 2015	3.8	(4.5)	6.3	10.8	(12.3)	15.9	7	12.2	(15.2)	21.7	35.7	(45.6)	62.7	8
		Charbonnier et al., 2014	14.0	(15.3)	15.5	35.8	(41.2)	46.7	4	7.2	(10.2)	15.2	23.9	(28.7)	42.7	57
	Arm flexion	Dal Maso et al., 2015	3.7	(5.2)	7.5	11.4	(16.3)	20.7	7	9.3	(12.5)	17.4	24.9	(33.6)	47.5	8
		Charbonnier et al., 2014	7.3	(8.6)	11.5	20.5	(22.3)	30.7	4	14.6	(21.0)	27.7	41.0	(56.8)	68.6	57
	Arm extension	Dal Maso et al., 2015	3.7	(5.0)	7.3	11.8	(15.0)	20.6	7	7.5	(8.5)	9.2	24.8	(27.8)	29.5	8
	Hair combing	Dal Maso et al., 2015	4.8	(5.2)	7.7	16.2	(20.7)	27.4	7	6.8	(10.0)	16.3	22.2	(34.3)	55.0	8
	Ball throwing	Dal Maso et al., 2015	4.3	(4.8)	6.8	15.3	(20.6)	26.6	7	34.4	(34.8)	36.9	110.5	(111.3)	111.7	8
	Eating	Dal Maso et al., 2015	5.2	(6.0)	6.5	16.0	(16.8)	18.2	7	6.8	(7.9)	12.8	20.9	(23.9)	37.6	8
	Gleno-humeral functional movement	Dal Maso et al., 2015	2.8	(2.9)	4.7	12.6	(13.0)	16.6	7	12.4	(13.5)	18.1	53.4	(54.3)	58.6	8
	Punching	Dal Maso et al., 2015	3.8	(4.5)	4.7	16.2	(18.5)	19.5	7	18.8	(19.0)	19.9	62.5	(63.4)	64.5	8
	Reaching the back	Dal Maso et al., 2015	4.8	(6.8)	9.2	13.6	(17.5)	25.9	7	5.5	(5.6)	7.1	18.3	(19.7)	23.7	8